HHS Public Access

Author manuscript

Neurobiol Dis. Author manuscript; available in PMC 2017 October 01.

Published in final edited form as:

Neurobiol Dis. 2016 October ; 94: 116–128. doi:10.1016/j.nbd.2016.06.010.

Maternal inflammation leads to impaired glutamate homeostasis and up-regulation of Glutamate Carboxypeptidase II in activated microglia in the fetal/newborn rabbit brain

Zhi Zhang[1], **Bassam Bassam**[1], **Ajit G. Thomas**[3], **Monica Williams**[1], **Jinhuan Liu**[1], **Elizabeth Nance**[1], **Camilo Rojas**[3], **Barbara S. Slusher**[2,3], and **Sujatha Kannan**[1]

[1]Department of Anesthesiology and Critical Care Medicine, Johns Hopkins School of Medicine, 1800 Orleans St, Baltimore, MD, 21287, USA

[2]Department of Neurology, Johns Hopkins School of Medicine, 1800 Orleans St, Baltimore, MD, 21287, USA

[3]Johns Hopkins Drug Discovery, Johns Hopkins School of Medicine, 1800 Orleans St, Baltimore, MD, 21287, USA

Abstract

Astrocyte dysfunction and excessive activation of glutamatergic systems has been implicated in a number of neurologic disorders, including periventricular leukomalacia (PVL) and cerebral palsy (CP). However, the role of chorioamnionitis on glutamate homeostasis in the fetal and neonatal brains is not clearly understood. We have previously shown that intrauterine endotoxin administration results in intense microglial ‘activation’ and increased pro-inflammatory cytokines in the periventricular region (PVR) of the neonatal rabbit brain. In this study, we assessed the effect of maternal inflammation on key components of the glutamate pathway and its relationship to astrocyte and microglial activation in the fetal and neonatal New Zealand white rabbit brain. We found that intrauterine endotoxin exposure at gestational day 28 (G28) induced acute and prolonged glutamate elevation in the PVR of fetal (G29, 1 day post-injury) and postnatal day 1 (PND1, 3 days post-injury) brains along with prominent morphological changes in the astrocytes (soma hypertrophy and retracted processes) in the white matter tracts. There was a significant increase in glutaminase and N-Methyl-D-Aspartate receptor (NMDAR) NR2 subunits expression along with decreased glial L-glutamate transporter 1 (GLT1) in the PVR at G29, that would promote acute dysregulation of glutamate homeostasis. This was accompanied with significantly decreased TGF-β1 at PND1 in CP kits indicating ongoing neuroinflammation. We also show for the first time that glutamate carboxypeptidase II (GCPII) was significantly increased in the activated microglia at the periventricular white matter area in both G29 and PND1 CP kits. This was confirmed by in vitro studies demonstrating that LPS activated primary microglia markedly upregulate GCPII enzymatic activity. These results suggest that maternal intrauterine endotoxin

Corresponding author: Sujatha Kannan, MD, Mailing address: Department of Anesthesiology and Critical Care Medicine, Charlotte Bloomberg Children’s Center 6318D, 1800 Orleans Street Baltimore, MD, 21287, Tel: 410- 955-6412 skannan3@jhmi.edu.

exposure results in early onset and long-lasting dysregulation of glutamate homeostasis, which may be mediated by impaired astrocyte function and GCPII upregulation in activated microglia.

Keywords

Cerebral palsy; periventricular leukomalacia; glutamate; glutamate carboxypeptidase II (GCPII); microglia; astrocytes; rabbit

Introduction

Neuroinflammation and glutamate excitotoxicity are common pathophysiologic mechanisms that are involved in perinatal/neonatal brain injury, including cerebral palsy (CP) (Vexler and Ferriero, 2001, Vannucci and Hagberg, 2004, Folkerth, 2005, Johnston, 2005, Johnston and Hoon, 2006, Leonardo and Pennypacker, 2009). Glutamate is the major excitatory neurotransmitter in the mammalian central nervous system and plays important roles in a variety of physiological and pathological functions (Choi, 1988). Glutamate is mainly produced from glutamine by glutaminase localized in neurons (Martinez-Hernandez et al., 1977, Erecinska and Silver, 1990, Westergaard et al., 1995), astrocytes (Cardona et al., 2014) and activated microglia/macrophages (Huang et al., 2011, Thomas et al., 2014). Glutamate can also be produced by the hydrolysis of N-acetylaspartylglutamate (NAAG), an abundant peptide neurotransmitter in the mammalian brain, into N-acetylaspartate (NAA) and glutamate by glutamate carboxypeptidase II (GCPII) that has been shown in several studies to be primarily localized to the astrocyte cell membrane in the central nervous system (CNS) (Robinson et al., 1987, Sacha et al., 2007) (Fig. 1A) and satellite cells and Schwann cells in the peripheral nervous system (Carozzi et al., 2008).

Glial cells, such as astrocytes and microglia, play important roles in both normal brain function and in injury (Vernadakis, 1996, Vesce et al., 1999, Grady et al., 2003, Kou and VandeVord, 2014). We have previously demonstrated that intrauterine infection with LPS induced microglial activation and pro-inflammatory cytokine release, which results in hypomyelination and motor deficits that persist even at PND5 (8 days after the insult) (Kannan et al., 2007, Saadani-Makki et al., 2008, Kannan et al., 2012, Balakrishnan et al., 2013) in the neonatal rabbits. The severity of the motor deficits correlated with the extent of microglial activation in the brain at birth as determined by in vivo imaging by positron emission tomography (PET) using the ligand [11C] PK11195 which is specific for activated microglia (Kannan et al., 2011a). We have also demonstrated the presence of neuronal injury in this model as evidenced by decreased neuronal counts in the thalamus (Kannan et al., 2012, Balakrishnan et al., 2013). The thalamic neuronal loss was associated with decreased dendrites and spines in the retrospenial cortex, a major projection site from the anterior thalamic neurons (Balakrishnan et al., 2013), as well as a decrease in the serotonin staining thalamocortical fibers in the parietal somatosensory cortex (Kannan et al., 2011b).

Studies show that activated macrophages and microglia release glutamate (Choi, 1988, Piani et al., 1992) and inflammation promotes glutamate release (Wan et al., 1994, al-Shabanah et al., 1996). Under normal circumstance, glutamate induces calcium influx through NMDARs to promote neuronal plasticity and survival (Citri and Malenka, 2008). However, under

pathological conditions, excessive extracellular glutamate causes over-activation of NMDARs, which results in neuronal damage (Choi, 1992) and initiates astrocyte pathology (Floyd et al., 2005).

The homeostasis of extracellular glutamate concentration is mainly controlled by astrocytes that play an important role in regulating glutamate formation and glutamate receptor function (Danbolt, 2001, McKenna, 2007, Kreft et al., 2012, Schousboe et al., 2014). Moreover, astrocytes play a crucial role in the clearance of extracellular glutamate to maintain glutamate homeostasis and restore low basal extracellular glutamate concentration, which is essential for ongoing neurotransmission and reducing neuronal cell death (Rothstein et al., 1996, Tanaka et al., 1997). Glutamate uptake and regulation by astrocytes is tightly associated with a multi protein complex which includes GLT-1 (Haugeto et al., 1996). GLT1 plays an important role in regulating glutamate concentration in the extracellular space to maintain normal synaptic function (Danbolt, 2001) and prevent excitotoxicity (Tanaka et al., 1997). GLT-1 level can be regulated by transforming growth factor-β1 (TGF-β1). Depletion of TGF-β1 results in a loss of GLT-1 and decreased glutamate uptake in the mouse hippocampus (Koeglsperger et al., 2013). TGF-β1is expressed by neuron and glial cells (Unsicker et al., 1991) and exerts a protective effect against various neuronal insults (Prehn et al., 1993, Flanders et al., 1998).

Most of the research on the role of glial cells in neuroinflammation and glutamate excitotoxicity has focused almost exclusively on adult neurodegeneration and neurological diseases [review (Sidoryk-Wegrzynowicz et al., 2011)]. The presence of astrogliosis in the white matter regions of the brain in periventricular leukomalacia has been demonstrated in several animal studies and human post-mortem studies (Leviton and Gilles, 1981, Sen and Levison, 2006, Pierson et al., 2007). In this study, the effects of maternal intrauterine inflammation on changes in astrocyte morphology along with glutamate receptor and enzyme expressions in the periventricular region of the brain over time after injury are evaluated. This study provides an initial foundation for further studies in exploring the link between neuroinflammation and glutamate excitotoxicity in neonatal and perinatal brain injuries. A better understanding of this will be crucial in determining novel therapeutic targets for brain injury following maternal intrauterine inflammation.

Materials and Methods

Animals

Time pregnant New Zealand white rabbits were ordered from Robinson Services Inc. (North Carolina, U.S.A.) and arrived at the facility one week before surgery. All animals were housed under ambient conditions (22°C, 50% relative humidity, and a 12-h light/dark cycle), and necessary precautions were undertaken throughout the study to minimize pain and stress associated with the experimental treatments. Experimental procedures were approved by the Johns Hopkins University Animal Care and Use Committee (IACUC).

Animal Model

After one week of acclimation, the pregnant rabbits were randomly divided into a control group (n=27 rabbits) and an endotoxin group (n= 30 rabbits), and underwent laparotomy at gestational day 28 (G-28). The endotoxin group received a total of 8,000 EU of LPS (E.coli serotype O127:B8, Sigma Aldrich, St Louis MO) in saline, that was equally divided and injected along the wall of the uterus as previously described (Saadani-Makki et al., 2008, Kannan et al., 2011b). Control group received an equal volume of saline injection. For the G29 study, the pregnant rabbits from control and endotoxin groups went through cesarean section on G29 and the kits were sacrificed and brains harvested. For the postnatal day 1 (PND1) study, the kits from control and endotoxin groups were born spontaneously on G31 (full term) and kept in incubators with the temperature of ~32–35°C and relative humidity of ~60–70% until sacrifice. Necessary precautions were undertaken throughout the study to minimize pain and stress associated with the experimental treatments.

Neurobehavior

Neurobehavioral tests were carried out on PND1 by personnel blinded to the experimental groups. Each animal was videotaped for 10 min and scored on a scale of 0–3 (0, worst; 3, best) for posture, movements of head and limbs, and duration and intensity of movements on a flat surface, as previously described for rabbits (Derrick et al., 2004, Zhang et al., 2015). The kits were fed with rabbit milk using a syringe attached to an artificial nipple and the suck and swallow were assessed on a scale of 0–3 (worst-best) (Derrick et al., 2004). The hops and steps were scaled at 0–4 (0, no step or hop; 4, ≥10 steps or 4 hops) (Kannan et al., 2012). Olfaction was tested by the intensity of aversive response to a cotton swab soaked with 100% ethanol (Georgiadis et al., 2008, Eixarch et al., 2012). The total possible behavioral score was 22 and cerebral palsy (CP) phenotypes were defined as: 0–6, severe; 6–12, moderate; 12–18 mild; 18–22, healthy.

Glutamate concentration

Kits from control and endotoxin groups were sacrificed at G29 and PND1. The brains were quickly harvested and the periventricular regions (PVR), including part of the corpus callosum, corona radiata, internal capsule, caudate and dorsal hippocampus, were micro-dissected and stored at −80°C until use. 50 mg of dissected tissue was homogenized in 500 μl lysis buffer (Promega, Madison, WI, USA) using a motorized homogenizer. The tissue weight was normalized to the lysis buffer volume such that for every mg of tissue 10uL of lysis buffer was used. This accounted for any minor variability in the weight between samples. After three frozen-thaw cycles, the tissue homogenate was centrifuged at 12,000xg for 20 min at 4°C and the supernatant was collected. The glutamate concentration was measured using Amplex Red Glutamic Acid/Glutamate Oxidase Assay Kit (Life Technologies, Grand Island, NY, USA) in 50 μl of the supernatant according to the manufacturer's instructions. The total tissue glutamate concentration, which includes the extracellular and intracellular glutamate, was expressed in mM.

Real-time PCR

Kits from control and endotoxin groups were sacrificed at G29 (control=8, from 5 litters; endotoxin=9, from 6 litters) and PND1 (control=8, from 7 litters; endotoxin=8, from 7 litters). The brains were quickly harvested and stored in RNAlater solution (Life technologies, Grand Island, NY, USA). The PVR were micro-dissected and the total RNA was extracted using TRIZOL (Life Technologies, Grand Island, NY, USA) according to the manufacturer instructions. RNA samples were quantified using the Nanodrop ND-1000 Spectrophotometer. The single-stranded complementary DNA (cDNA) was first reverse transcribed from the total RNA samples using the High Capacity cDNA Reverse Transcription Kit with RNase inhibitor (Life Technologies, Grand Island, NY, USA). The real-time PCR was performed with Power SYBR Green PCR Master Mix (Life Technology, Grand Island, NY, USA) using Fast 7500 Real-time PCR systems (Life Technologies, Grand Island, NY, USA). Amplification conditions included 30 min at 48°C, 10 min at 95°C, 40 cycles at 95°C for 15 s and 60°C for 1 min. List of primers and their specifications are described in Table 1. Primers were custom designed and ordered from Integrated DNA technology (Iowa, USA). Comparative Ct method was used to assess differential gene expressions between control and endotoxin groups at different time points. The gene expression levels for each sample were normalized to its expression level of the housekeeping gene encoding glyceraldehyde 3-phosphate dehydrogenase (GAPDH) (ΔCt); the difference between the endotoxin group and the control group was used to determine the ΔΔCt. The $2^{-\Delta\Delta Ct}$ gave the relative fold changes in gene expression between control and endotoxin animals

Western blot

Kits from control and endotoxin groups were sacrificed at G29 (control=8, from 4 litters; endotoxin=9, from 7 litters) and PND1 (control=8, from 8 litters; endotoxin=9, from 8 litters). Total protein was isolated from the PVR brain tissues using RIPA solution (100 mg brain tissue/1 ml RIPA solution) (Cell Signaling, Danvers, MA, USA) according to the manufacturer's instructions. Protein concentration was determined by using the BCA kit (ThermoFisher Scientific, Waltham, MA, USA). 20 μg of protein was run on the precast NuPAGE 4–12% Bis-Tris gel (Life Technologies, Grand Island, NY, USA) and transferred on the nitrocellulose membrane using iBlot® Transfer Stack (Life Technologies). After blocking, the membranes were incubated with mouse anti-GLT-1 (1:500, Novus Biologicals, Littleton, CO, USA). Membranes were washed and then incubated with goat anti-mouse IgG H&L (HRP) (Abcam, Cambridge, MA, USA). β-actin (ThermoFisher Scientific) was used as an endogenous control to normalize the loading and compare the expression of target proteins between different groups. Membranes were developed with Amersham ECL western blotting detection reagents (GE healthcare, Pittsburgh, PA, USA). Gel images were scanned and analyzed by using ImageJ software.

Immunohistochemistry

The rabbits were anesthetized and transcardially perfused with saline at G29 (control=5 kits, from 3 litters; endotoxin=7 kits, from 4 litters) or PND1 (control=7 kits, from 7 litters; endotoxin=5 kits, from 3 litters), followed by 4% paraformaldehyde (PFA) in PBS. The

brains were removed and post-fixed in 4% PFA overnight and cryoprotected in graded sucrose solutions. Coronal sections (30 μm, 1:6 series) were incubated in 0.3% hydrogen peroxide (H_2O_2) solution, blocked by 3% normal goat serum in 0.1 M phosphate-buffered saline (PBS). Sections were then incubated overnight at 4°C with chicken anti-GFAP (1:500, abcam, MA. U.S.A.) or mouse anti-GCPII (1:250, GeneTex, CA, U.S.A.). Sections were subsequently washed and incubated with biotinylated secondary antibodies (1:250; Vector Laboratories, Burlingame, CA) for 4 h at room temperature. Next, the sections were incubated for 2 h in avidin–biotin substrate (ABC kit, Vector Laboratories, Burlingame, CA). All sections were then incubated for 2 min in 3,30-diaminobenzidine (DAB) solution (Vector Laboratories). Sections were dehydrated in ethanol and Histo-Clear™ II (Fisher Scientific, Pittsburg, PA, U.S.A.), and cover-slipped using mounting medium. Co-localization of IBA1/GCPII and GFAP/GCPII were done by incubating the sections overnight at 4°C with chicken anti-GFAP (1:250, abcam, MA. U.S.A.)/mouse anti-GCPII (1:200, GeneTex, CA, U.S.A.), or goat anti-IBA1 (1:250, abcam, MA. U.S.A.)/mouse anti-GCPII (1:200, GeneTex, CA, U.S.A.). Sections were subsequently washed and incubated with fluorescent secondary antibodies (1:250; Life Technologies, MA, U.S.A.) for 2 h at room temperature. Next, the sections were incubated with DAPI (1:1000, Invitrogen) for 15 min. After wash, the slides were dried and cover slipped with mountain medium (Dako, Carpinteria, CA, USA). Confocal images were acquired with Zeiss ZEN LSM 710 (Zeiss, CA, U.S.A.) and processed with ZEN software.

Area measurement of glutamate carboxypeptidase II (GCPII)

Brain sections from control and endotoxin kits at G29 (control=5 kits, from 3 litters; endotoxin=7 kits, from 4 litters) and PND1 (control=7 kits, from 7 litters; endotoxin=5 kits, from 3 litters) were stained with GCPII antibody. All slides and images were coded and the analysis was performed with personnel blinded to the experiments. Images (40X, 4–5 images/brain region/animal) were randomly acquired from corpus callosum and internal capsule regions using Nikon Eclipse 90i and Stereo Investigator software (MBF Bioscience, Williston, VT, U.S.A.). The percentage of area of GCPII expressions were measured using particle analysis function in ImageJ software according to the software instructions. In brief, the images were converted to 8-bit greyscale and the threshold was manually adjusted followed by application of the ‘analyze particles’ function with the size parameters (pixel units) of 0.0001–infinity and circularity 0–1 (show outlines). The optimum parameters were identified by manually tracing using “freehand” tool on one image and systematically varying one parameter at a time while fixing all other parameters to avoid detecting artefacts. Once the optimal parameters had been determined, these were applied to all images, threshold being the only user-dependent parameter for this method. Finally, a visual check was performed utilizing the ‘merge channel” function in ImageJ, which merges the outline of the measured areas with the original image, to show the maximum merging of images. The percentage area were averaged and compared between control and endotoxin groups.

Fluorescence intensity measurement

Brains from control and endotoxin kits at G29 (control=5 kits, from 2 litters; endotoxin=4 kits, from 3 litters) and PND1 (control=6 kits, from 4 litters; endotoxin=5 kits, from 3 litters)

were collected. Coronal sections from the bregma to the dorsal hippocampus (30 μm of thickness, 180 μm apart) were co-stained with GCPII and IBA1 antibody, and incubated with fluorescent secondary as described previously. All slides and images were coded and the analysis was performed with personnel blinded to the experiments. Confocal images (63X, 9–12 images/brain region/animal) were randomly acquired from corpus callosum and internal capsule regions using Zeiss ZEN LSM 710 (Zeiss, CA, U.S.A.). The camera settings were kept the same during image acquirement. The confocal images were exported into green (IBA1), red (GCPII) and blue (DAPI) fluorescence channels using ZEN2 (blue edition) software (Zeiss, CA, U.S.A.). The green (IBA1) and red fluorescent (GCPII) images were loaded into MCID™ Core software (MCID Image Analysis Software Solutions for Life Science). The fluorescence intensity of the IBA1 and GCPII in the same microglial cells were measured using MCID™ Core software according the manufacturer's instructions. Microglial cells (IBA1) were delineated in the green channel and redirected sampling was used to measure fluorescence within this area in the red channel (GCPII). The fluorescence intensity of IBA1, GCPII and the ratio of GCPII/IBA1 fluorescence intensity of individual microglial cells were calculated, averaged and compared between control and endotoxin kits.

Cell culture and treatment

Cells were obtained from confluent mixed glial cultures (10–21 days in vitro) of Sprague-Dawley 1–2 day old pup brains following the method developed previously (Giulian and Baker, 1986). Cells were treated in serum and phenol red-free medium (DMEM) for 24 h with/without LPS (1 μg/mL) and the GCPII inhibitor 2-phosphonomethyl pentanedioic acid (2-PMPA) (1 μM). Cell lysates were collected and GCPII enzymatic activity was quantified.

GCPII enzyme activity assay

The GCPII activity assay was carried out as previously described (Rojas et al., 2002). Briefly, the reaction mixture contained NAA[3H]G (20 nM, 4.3 nmol/μCi), GCPII source, either purified recombinant human GCPII (5–300 pM) for positive controls (Barinka et al., 2002) or cell lysate in Tris–HCl (pH 7.4, 40 mM) containing CoCl2 (1 mM), in a total volume of 50 μL. The reaction was carried out at 37 °C for 1h and stopped with ice-cold sodium phosphate buffer (pH 7.5, 0.1 M, and 50 μL). An aliquot of the reaction mixture (90 μL) was transferred to a 96-well spin column containing AG1X8 ion-exchange resin; the spin column was centrifuged at 900 rpm for 3–5 min using a Beckman GS-6R centrifuge equipped with a PTS-2000 rotor. NAA[3H]G bound to the resin and [3H]G eluted in the flow through. The columns were then washed twice with formate (1 M, 90 μL) to ensure complete elution of [3H] G. The flow through and the washes were collected in a deep 96-well block; an aliquot (200 μL) was transferred to a solid scintillator-coated 96-well plate (Packard) and dried to completion. The radioactivity corresponding to [3H] G was determined with a scintillation counter (Topcount NXT, Packard, counting efficiency 40%). Assay points for each experiment were the average of 6–8 determinations.

Area measurement of GFAP expression

Brain sections from control and endotoxin kits at G29 (control=5 kits, from 3 litters; endotoxin=7 kits, from 4 litters) and PND1 (control=7 kits, from 7 litters; endotoxin=5 kits,

from 3 litters) were stained with GFAP antibody. All slides and images were coded and the analysis was performed with personnel blinded to the experiments. Images (40X, 4–5 images/brain region/animal) were randomly acquired from corpus callosum and internal capsule regions using Nikon Eclipse 90i and Stereo Investigator software (MBF Bioscience, Williston, VT, U.S.A.). The percentage area of GFAP expression was measured using particle analysis function in ImageJ software as described above. The percentage area were averaged and compared between control and endotoxin groups.

Astrocytes reconstruction and morphological analysis

Brain sections from control and endotoxin kits at G29 (control=5 kits, from 3 litters; endotoxin=7 kits, from 4 litters) and PND1 (control=7 kits, from 7 litters; endotoxin=5 kits, from 3 litters) were stained with GFAP antibody. All slides and images were coded and the analysis was performed with the personnel blinded to experiments. Images (40X, 4–5 images/brain region/animal) were randomly acquired from corpus callosum and internal capsule regions using Nikon Eclipse 90i and Stereo Investigator software (MBF Bioscience, Williston, VT, U.S.A.). Astrocytes to be traced (40X, 2–3 cells/image) were chosen at random from the corpus callosum and internal capsule regions from control and endotoxin kits at G29 and PND1. The astrocytes that met the following criteria were traced: (1) Cell body located in the corpus callosum and internal capsule; (2) Processes are completely contained within the slice; (3) Cells sufficiently stained to allow for tracing processes. The soma morphology and processes of the astrocytes were analyzed using the Neurolucida Explorer software package (MBF Bioscience, Williston, VT, U.S.A.).

Statistical analysis

All data were processed with GraphPad Prism. Data were presented as mean values ± S.E.M. with the exception of the neurobehavioral data, which were expressed as Median with range. Two-tail unpaired t-test was used for group comparisons. Statistical significance was set at $p<0.05$ for all analyses.

Results

Endotoxin kits had severe CP phenotype

For the G29 study, the kits in the control and endotoxin groups were collected by C-section and sacrificed immediately. For the PND1 study, we assessed the kits phenotype with neurobehavioral tests on PND1. The kits from the endotoxin group exhibited a severe CP phenotype with crossing of hind limbs, hindlimb hypertonia, and poor motor function as demonstrated by individual scores of 0–1 and total behavioral scores <6 (posture, suck and swallow, head and limb movements, steps, and aversive response to alcohol, Table 2).

Elevated glutamate level in the periventricular region in endotoxin kits

Although glutamate is abundant in the brain, only a fraction of it is present extracellularly at concentrations of 1–10 μM (Hamberger and Nystrom, 1984); while, intracellular glutamate concentration is several thousand-fold higher (Ottersen et al., 1992). Intracellular glutamate is generally considered non-toxic, while high concentrations of extracellular glutamate are toxic due to the excessive activation of glutamate receptors (Choi, 1987). We measured the

total tissue glutamate level, which includes both intracellular and extracellular glutamate, in the PVR from control and endotoxin kits at G29 and PND1. We found that the glutamate level was significantly increased at G29 in endotoxin kits (n=9, from 5 litters) when comparted to control kits (n=5, from 1 litters) [$t_{(12)}$=2.7, p=0.02]. The elevated glutamate level was persistent at P1 in endotoxin kits (n=9, from 7 litters) compared with control kits (n=8, from 5 litters) [$t_{(15)}$=2.2, p=0.04] (Fig. 1B).

Increased glutaminase and NMDARs mRNA levels in CP kits

We measured the mRNA expressions of glutaminase and NMDARs in the PVR on G29 and PND1. In humans, glutaminases are encoded by two paralogous genes, glutaminase [kidney-type (K) isozyme] (Mock et al., 1989, Mates et al., 2013) and glutaminase2 [liver-type (L) isozyme], located in distinct chromosomes (Aledo et al., 2000, Olalla et al., 2002, Marquez et al., 2013). We found that the glutaminase2 mRNA expression in the PVR was significantly increased [$t_{(15)}$=3.0, p=0.009] at G29 (1 day after injury), while there was no significant difference in the glutaminase mRNA expression [$t_{(15)}$=0.6, p=0.6]. The mRNA expressions of glutaminase [$t_{(14)}$=2.2, p=0.048] and glutaminase2 [$t_{(14)}$=3.6, p=0.003] were significantly decreased at PND1 (3 days after injury) (Fig. 2A, B).

NMDAR signaling is involved in cell death, survival and plasticity (Hardingham and Bading, 2003). Calcium influx through NMDA receptors is responsible for the excitotoxicity (Choi, 1987) and is implicated in a variety of neurological conditions (Dong et al., 2009). We measured the NR2A and NR2B subunits of NMDA receptors and found that the mRNA levels of NR2A [$t_{(15)}$=3.2, p=0.006] and NR2B [$t_{(15)}$=2.3, p=0.04] were significantly increased in the endotoxin kits at G29, compared with control kits. There was a significant decrease in NR2B [$t_{(14)}$=2.9, p=0.01], with no difference in the NR2A [$t_{(14)}$=0.7, p=0.5] mRNA levels in the endotoxin kits at PND1, compared with control kits (Fig. 2C, D). The decreased mRNA expression of glutaminase enzyme and NMDAR NR2 subunits on PND1 may be attributed to the neuronal loss that has been shown in this model previously or it may be due to a compensatory response to the elevated glutamate levels that persists even 3 days after injury (PND1).

Decreased GLT-1 protein level in CP kits

GLT-1 is a major transporter of glutamate in the brain, which plays an important role in regulating extracellular glutamate concentration (Danbolt, 2001) and preventing excitotoxicity (Tanaka et al., 1997). We measured GLT-1 protein levels at G29 and PND1 using Western blot. We found that the GLT-1 level was significantly decreased in endotoxin kits at G29 [$t_{(15)}$=3.2, p=0.006], but came back up to control levels by PND1 [$t_{(15)}$=0.1, p=0.9] (Fig. 2E).

Decreased TGF-β1 mRNA level in CP kits

TGF-β 1 regulates cellular physiology, such as cell growth (Henrich-Noack et al., 1996), mediates pathophysiological processes, such as inflammation and tissue repair (Roberts et al., 1990), modulates both excitatory and inhibitory synaptic transmission in the adult mammalian brain (Krieglstein et al., 2011) and attenuates microglial activation and promotes an anti-inflammatory phenotype in resting and activated microglia (Norden et al., 2014). We

measured the TGF-β1 mRNA levels in the PVR on G29 and PND1. We found that there was no change in the TGF-β1 level at G29 [$t_{(15)}$=1.8, p=0.1], however, the TGF-β1 level significantly decreased at PND1 [$t_{(14)}$=2.3, p=0.04] (Fig. 2F).

GCPII enzyme activity and expression in the white matter area in CP kits

GCPII is a transmembrane peptidase that cleaves NAAG to free glutamate in the synaptic cleft (Robinson et al., 1987). GCPII is present in membrane and cytosolic fractions (Barinka et al., 2002). We measured GCPII activity, which included both the membrane and cytosolic fractions, in the PVR of the brains from PND1 kits (control=5, from 3 litters; endotoxin=4, from 4 litters). We found that the GCPII enzyme activity in PVR was similar in both the control and the endotoxin kits [$t_{(7)}$=0.8, p=0.4] (Fig. 3B). However, regional protein expression, as determined by immunohistochemistry staining for GCPII, demonstrated significantly increased GCPII expression in CP kits in the corpus callosum [$t_{(30)}$=2.1, p=0.04] at G29, and a significant increase in GCPII expression in the internal capsule [$t_{(29)}$=2.3, p=0.03] at PND1, when compared to age matched controls (Fig. 3A, C and D).

Co-localization of GCPII with astrocytes and activated microglia

GCPII has been previously shown to be primarily expressed in astrocytes. Due to the increased GCPII staining in the periventricular white matter regions in the endotoxin kits, the cellular localization of GCPII in these regions was evaluated and compared between control and endotoxin kits. We co-stained GFAP/GCPII and IBA1/GCPII and analyzed the co-localization of GCPII with astrocytes and/or microglia on G29 and PND1. We found that GCPII was mainly co-localized with astrocytes in both control and endotoxin kits on G29 and PND1 (Fig. 4A–D). However, GCPII was also found to co-localize with activated microglia in CP kits at both time points (Fig. 4E–H).

GCPII is significantly upregulated in the activated microglial cells at the PVR in the endotoxin kits

To verify up-regulation of GCPII in activated microglia, brain sections from control and endotoxin kits were co-stained with IBA1 and GCPII. The fluorescence intensity of IBA1, GCPII in the IBA1 labelled cells, and the ratio of GCPII/IBA1 in the same microglial cells in the corpus callosum and internal capsule were calculated, averaged and compared between control and endotoxin kits at G29and PND1. We found that the IBA1 fluorescence intensity was increased in corpus callosum [G29: $t_{(516)}$=7.22, p<0.001; PND1: $t_{(740)}$=4.87, p<0.001] and internal capsule [G29: $t_{(228)}$=7.50, p<0.001; PND1: $t_{(608)}$=7.60, p<0.001] in the endotoxin kits (Fig. 5A–D, G). Along with this, the GCPII fluorescent intensity in the microglial cells was markedly upregulated in the corpus callosum [G29: $t_{(516)}$=16.09, p<0.001; PND1: $t_{(740)}$=24.86, p<0.001] and internal capsule [G29: $t_{(228)}$=16.77, p<0.001; PND1: $t_{(608)}$=28.33, p<0.001] in the endotoxin kits (Fig. 5E, H) when compared to controls. This was further confirmed by the ratio of GCPII/IBA1 which was significantly higher in corpus callosum [G29: $t_{(516)}$=9.59, p<0.001; PND1: $t_{(740)}$=17.55, p<0.001] and internal capsule [G29: $t_{(228)}$=4.70, p<0.001; PND1: $t_{(608)}$=9.82, p<0.001] in the endotoxin kits (Fig. 5F,I), indicating that the increase in GCPII expression was due to upregulation of the protein and not just due to proliferation or increase in microglial cells.

GCPII is markedly upregulated in microglial cells activated by LPS

To ascertain if GCPII is upregulated in activated microglia, rat primary microglial cells were treated with and without 1μg/mL of LPS and GCPII enzymatic activity was quantified in the cell lysates upon hydrolysis of its substrate NAA[^{3}H]G, that was added exogenously. GCPII activity was strongly up-regulated in rat primary microglia activated by LPS while it was very low in the cells that were not exposed to LPS. GCPII activity was suppressed by co-treatment with 2-PMPA, a small molecule inhibitor of GCPII (Fig. 5J). This indicates that GCPII is constitutively expressed at low levels in normal, resting microglia but is significantly upregulated in microglia activated by LPS exposure. This is similar to what we see in vivo where GCPII co-localization and expression in microglia was significantly higher in the endotoxin kits compared to age matched controls.

Changes in the astrocyte morphology

Since astrocytes play a major role in glutamate homeostasis and since GCPII is located on the membrane of astrocytes, we also evaluated the changes in the astrocyte morphology in the PVR of the endotoxin and control kits both prenatally and at term. Brain sections from control and endotoxin kits at G29 and PND1 were stained for GFAP and percentage area with GFAP expression/staining in the corpus callosum and internal capsule was compared between the two groups. There was no difference in the percentage of area stained between the control and endotoxin exposed kits (Fig. 6A, B, C). However, a significant change in morphology indicated by an increase in the area of the soma, along with decrease in the length of processes and number of nodes was noted in the corpus callosum [$t_{(51)}$=4.5, $p<0.001$, $t_{(51)}$=4.9, $p<0.001$ and $t_{(51)}$=5.7, $p<0.001$, respectively] and internal capsule [$t_{(55)}$=3.3, $p=0.002$, $t_{(55)}$=4.2, $p<0.001$ and $t_{(55)}$=5.5, $p<0.001$, respectively] at G29, with persistence in the decreased process length [$t_{(69)}$=3.3, $p=0.002$] and decreased process nodes [$t_{(69)}$=2.5, $p=0.02$] seen in the internal capsule even three days after the intrauterine insult at PND1 (Fig 6A, D–I).

Discussion

In this study, using a previously established rabbit model of maternal inflammation induced cerebral palsy, we evaluated the role of intrauterine endotoxin exposure on the progression of glutamate pathway dysregulation and astrocyte dysfunction in the fetal and neonatal brains. We have previously shown that this model results in a robust increase in microglial proliferation and increase in pro-inflammatory cytokines in the periventricular region of newborn rabbit brain that peaks at PND1 and persists until PND5 (Kannan et al., 2007, Kannan et al., 2012). The periventricular region (PVR) is the classic area that is affected in patients with cerebral palsy and in perinatal/neonatal brain injury. This area also corresponds to the region where maximal microglial proliferation and ‘activation’ occurs in this model following an insult and in other models of periventricular leukomalacia (Kannan et al., 2007, Saadani-Makki et al., 2008, Falahati et al., 2013). Microglial cells are present in the PVR in preterm infants and activated glia are increased in numbers in those with periventricular white matter injury (Verney et al., 2012). Since glial activation may be responsible in part for the glutamate mediated excitotoxicity, we focused on those areas (PVR) where glial activation is typically seen in perinatal brain injury. Here, we show that intrauterine

inflammation results in acute dysregulation of glutamate homeostasis along with changes in astrocyte morphology in the PVR that is predominant in the fetal brain at G29 (1 day post-injury), as evidenced by the significantly elevated glutamate levels, increased glutaminase and NR2A and NR2B expression, as well as decreased GLT-1 levels at this age. This increase in total glutamate level measured in the brain persists even at PND1 (3 days post-injury) in the newborn rabbit kits with severe CP phenotype. This is in spite of the decrease in mRNA expression of glutaminase and NMDAR, and normalization of GLT-1 expression by PND1. This paradox may be explained in part by the increased GCPII in activated microglia along with persistent abnormalities in astrocyte morphology in areas such as the internal capsule that may indicate an inability to compensate for the initial glutamate toxicity. The decreased mRNA of glutaminase and NR2 NMDARs may be secondary to neuronal loss that has been described previously by our group in this model (Balakrishnan et al., 2013) or may represent a compensatory response to higher glutamate levels.

Glutamate-mediated excitotoxicity causes extensive damage to the developing brain in animal models of hypoxia/ischemia (Silverstein et al., 1986). GCPII, previously called N-acetyl-α-linked acidic dipeptidase or NAALADase, catalyzes the hydrolysis of the neuropeptide NAAG to NAA and glutamate (Robinson et al., 1987, Stauch et al., 1989, Serval et al., 1990, Slusher et al., 1992, Fuhrman et al., 1994, Berger et al., 1999). Previous studies have demonstrated that GCPII is expressed in astrocytes in the CNS. Our study is the first one to demonstrate that LPS exposure induces upregulation of GCPII *in vivo* in activated microglia in the PVR in kits with CP, and *in vitro* in LPS activated primary microglial cells. Increased GCPII levels may play an important role in producing pathogenic levels of glutamate. In this case, although the overall GCPII enzyme activity did not change between control and endotoxin kits at PND1, the upregulation of GCPII protein levels specifically in activated microglia can lead to increased glutamate production in the PVR in endotoxin kits. We have previously shown in our model that there is increase in activated microglia, decreased microglial mobility and increased pro-inflammatory cytokine formation in the PVR (Saadani-Makki et al., 2008, Kannan et al., 2011a, Kannan et al., 2012, Zhang et al., 2016). One of the mechanisms by which neuoinflammation may lead to ongoing injury is through glutamate dysregulation. Although it is possible that glutamate formation from NAAG hydrolysis alone may not be enough to lead to the substantial increase in glutamate concentration noted here, increased GCPII expression may worsen the injury in multiple ways, one of which may be by decreasing the levels of neuroprotective NAAG. NAAG activates mGluR3 which plays a strong role in inhibiting presynaptic glutamate release (Hovelso et al., 2012). Since we have measured total glutamate in this study, we do not know what fraction of this glutamate is extracellular. Future studies using microdialysis may help in distinguishing and characterizing this further. GCPII or NAALADase expressed in other peripheral organs and in tumors/neovasculature has been shown to increase glutamate levels by mechanisms other than NAAG hydrolysis, such as hydrolysis of γ linked glutamyl folates and laminin peptides (Conway et al., 2013). However, this function has only been reported in peripheral organs and not in the CNS yet (Foss et al., 2012), therefore it is probably not a likely source of excess glutamate in the PVR in this model.

Another neuroprotective function of NAAG involves its role in regulating inflammation through its effect on astrocytes. Reactive astrocytes exert both pro- and anti-inflammatory functions at different locations and at different times in response to injury and during repair (Eddleston and Mucke, 1993, John et al., 2003). Astrocytes can modulate microglia activation (von Bernhardi and Ramirez, 2001, Min et al., 2006, Cerbai et al., 2012) and exert both pro- and anti-inflammatory effects on microglia (Min et al., 2006, Farina et al., 2007). NAAG binds to mGluR3 on astrocytes and can increase TGF-β1 release (Slusher et al., 1999, Thomas et al., 2001). Astrocyte-derived TGF-β1 inhibits microglial activation (Endo et al., 2015) and promotes a 'resting' or 'normal' microglial phenotype (Butovsky et al., 2014). TGF-β1 attenuates cytokine, chemokine, adhesion molecule and reactive oxidative species (ROS) production (Lodge and Sriram, 1996, Brionne et al., 2003, Paglinawan et al., 2003, Smith et al., 2013). Decreased TGF-β1 is known to contribute to a more pro-inflammatory micro-environment and can decrease the mobility of microglia (De Simone et al., 2010), as seen in our model (Zhang et al., 2016). The decreased TGF-β1 in the PVR in our study may imply the dysfunction of white matter astrocytes and contribute to the persistent pro-inflammatory and 'activated' state of microglia in the PVR that has been demonstrated previously by us in this rabbit model of CP (Kannan et al., 2007, Saadani-Makki et al., 2009, Kannan et al., 2012). Therefore, the astrocyte changes, GCPII upregulation and glutamate dysregulation demonstrated in the acute phase in this study may influence the function of microglia in the white matter tracts leading to the persistent neuro-inflammation seen in our model.

In our study, we found that administration of 2-PMPA, a specific GCPII inhibitor, reduced GCPII activity in LPS exposed microglia. Inhibition of GCPII could provide neuroprotective effects against excitotoxicity by reducing the production of extracellular glutamate (Slusher et al., 1999) both by decreasing liberation of glutamate from NAAG and by increasing NAAG concentrations which activates mGluR3 (Neale, 2011) and decreases presynaptic glutamate release (Wroblewska et al., 1997, Bruno et al., 1998b, Zuo et al., 2012). NAAG has also been shown to prevent NMDA-induced neuronal death (Puttfarcken et al., 1993, Valivullah et al., 1994, Khacho et al., 2015), and induce TGF-β release via activation of Mitogen-activated protein kinases (MAPK) and phosphoinositide 3-kinase (PI3K) (Bruno et al., 1998a, D'Onofrio et al., 2001). This may explain the neuroprotective effects of GCPII inhibition and NAAG administration in several adult models of neuroinflammation (Ghadge et al., 2003, Thomas et al., 2003, Rahn et al., 2012) and in hypoxic-ischemia (Slusher et al., 1999, Cai et al., 2002).

Under physiological conditions, astrocytes maintain homeostasis of extracellular glutamate (Mazzanti et al., 2001), provide metabolic substrates for neurons (Kasischke et al., 2004), regulate cerebral blood flow (Mulligan and MacVicar, 2004) and control synapse formation (Ullian et al., 2001). Under pathological conditions, astrocytes are activated (Chen and Swanson, 2003, Barreto et al., 2011) and react to injury by cellular hypertrophy, proliferation and increasing GFAP expression (Burns et al., 2009, Schachtrup et al., 2010, Sofroniew and Vinters, 2010). In a rodent model of diffuse white matter injury, chronic perinatal hypoxia delayed astrocyte maturation and compromised astrocyte function, as indicated by the decreased glial-specific glutamate transporter expression and function (Raymond et al., 2011). In our study, we found that there was significant decrease in the

GLT-1 protein level at G29, suggesting impaired glutamate uptake by astrocytes, which may increase the synaptic glutamate concentration and cause prolonged glutamate receptor activation and glutamate excitotoxicity. The GLT-1 level returned to normal at PND1, however, whether inflammation induces functional changes in GLT-1 needs to be further investigated.

In this study, we found that the expression of GFAP was similar between the control and CP kits, indicating no astrocyte proliferation. However, there were significant changes in the astrocyte morphology in the endotoxin kits compared to controls. An increase in the size of the soma along with a decrease in process length and nodes were seen in both the corpus callosum and internal capsule, indicating inflammation-induced astrocyte activation in the white matter. The morphological changes persisted (decreased process length and nodes) in the internal capsule at PND1, indicating ongoing astrocyte activation three days after the insult. These structural changes could be a direct result of the injury and/or the insult, or a compensatory mechanism to the injury or both. However, the presence of increased glutamate, along with decreased GLT-1, decreased TGF β and persistent microglial activation indicate that the changes in astrocyte morphology may indicate a negative effect or an inability of the astrocytes to adequately compensate for the increased glutamate and these effects may continue in some of these regions for a longer time period.

Studies demonstrate that diffuse innate immune activation (e.g. system bacterial infections) can induce mild or moderate reactive astrogliosis, which results in variable GFAP up-regulation (Sofroniew, 2009), variable hypertrophy of soma and processes in individual astrocytes (Wilhelmsson et al., 2006). Moreover, hypoxia ischemia injury induces astrocytes cell death and reduces GFAP-positive cell density in newborn piglets (Martin et al., 1997) and little or no astrocyte proliferation in human cerebral palsy patients (Villapol et al., 2008). Our results are consistent with these previous studies. These results are also in accordance with our previous studies where we found the greatest changes in parallel diffusivity and fractional anisotropy on diffusion tensor imaging, in the corpus callosum and internal capsule in newborn rabbits (Kannan et al., 2007). The decreases in parallel diffusivity and fractional anisotropy can be explained by the changes in astrocyte and microglial morphology seen in the white matter tracts. (Kannan et al., 2007, Kannan et al., 2009).

In summary, our study demonstrates that normal glutamate homeostasis is dysregulated in a complex manner by involvement of several pathways over time and this may in turn trigger and promote the persistent pro-inflammatory state that is seen in the neonatal brain following exposure to intrauterine inflammation even after removal from the maternal environment (Saadani-Makki et al., 2009, Kannan et al., 2012). Neuroinflammation induced upregulation of GCPII in activated microglia may play an important role in glutamate excitotoxicity. Thus, GCPII inhibition can decrease glutamate release and promote the release of endogenous TGF-β1 which may provide additional methods of modulating the neuroinflammatory response as a therapeutic intervention following neonatal brain injury.

Acknowledgments

This work is supported in part by the Eunice Kennedy Shiver NICHD, NIH, R01HD069562 (SK) and the R01CA161056 and P30MH075673 (BSS).

References

al-Shabanah OA, Mostafa YH, Hassan MT, Khairaldin AA, al-Sawaf HA. Vitamin E protects against bacterial endotoxin-induced increase of plasma corticosterone and brain glutamate in the rat. Res Commun Mol Pathol Pharmacol. 1996; 92:95–105. [PubMed: 8733831]

Aledo JC, Gomez-Fabre PM, Olalla L, Marquez J. Identification of two human glutaminase loci and tissue-specific expression of the two related genes. Mamm Genome. 2000; 11:1107–1110. [PubMed: 11130979]

Balakrishnan B, Dai H, Janisse J, Romero R, Kannan S. Maternal endotoxin exposure results in abnormal neuronal architecture in the newborn rabbit. Dev Neurosci. 2013; 35:396–405. [PubMed: 23988854]

Barinka C, Rinnova M, Sacha P, Rojas C, Majer P, Slusher BS, Konvalinka J. Substrate specificity, inhibition and enzymological analysis of recombinant human glutamate carboxypeptidase II. J Neurochem. 2002; 80:477–487. [PubMed: 11905994]

Barreto G, White RE, Ouyang Y, Xu L, Giffard RG. Astrocytes: targets for neuroprotection in stroke. Cent Nerv Syst Agents Med Chem. 2011; 11:164–173. [PubMed: 21521168]

Berger UV, Luthi-Carter R, Passani LA, Elkabes S, Black I, Konradi C, Coyle JT. Glutamate carboxypeptidase II is expressed by astrocytes in the adult rat nervous system. J Comp Neurol. 1999; 415:52–64. [PubMed: 10540357]

Brionne TC, Tesseur I, Masliah E, Wyss-Coray T. Loss of TGF-beta 1 leads to increased neuronal cell death and microgliosis in mouse brain. Neuron. 2003; 40:1133–1145. [PubMed: 14687548]

Bruno V, Battaglia G, Casabona G, Copani A, Caciagli F, Nicoletti F. Neuroprotection by glial metabotropic glutamate receptors is mediated by transforming growth factor-beta. J Neurosci. 1998a; 18:9594–9600. [PubMed: 9822720]

Bruno V, Wroblewska B, Wroblewski JT, Fiore L, Nicoletti F. Neuroprotective activity of N-acetylaspartylglutamate in cultured cortical cells. Neuroscience. 1998b; 85:751–757. [PubMed: 9639269]

Burns KA, Murphy B, Danzer SC, Kuan CY. Developmental and post-injury cortical gliogenesis: a genetic fate-mapping study with Nestin-CreER mice. Glia. 2009; 57:1115–1129. [PubMed: 19115384]

Butovsky O, Jedrychowski MP, Moore CS, Cialic R, Lanser AJ, Gabriely G, Koeglsperger T, Dake B, Wu PM, Doykan CE, Fanek Z, Liu L, Chen Z, Rothstein JD, Ransohoff RM, Gygi SP, Antel JP, Weiner HL. Identification of a unique TGF-beta-dependent molecular and functional signature in microglia. Nat Neurosci. 2014; 17:131–143. [PubMed: 24316888]

Cai Z, Lin S, Rhodes PG. Neuroprotective effects of N-acetylaspartylglutamate in a neonatal rat model of hypoxia-ischemia. Eur J Pharmacol. 2002; 437:139–145. [PubMed: 11890901]

Cardona C, Sanchez-Mejias E, Davila JC, Martin-Rufian M, Campos-Sandoval JA, Vitorica J, Alonso FJ, Mates JM, Segura JA, Norenberg MD, Rama Rao KV, Jayakumar AR, Gutierrez A, Marquez J. Expression of Gls and Gls2 glutaminase isoforms in astrocytes. Glia. 2014

Carozzi VA, Canta A, Oggioni N, Ceresa C, Marmiroli P, Konvalinka J, Zoia C, Bossi M, Ferrarese C, Tredici G, Cavaletti G. Expression and distribution of ‘high affinity’ glutamate transporters GLT1, GLAST, EAAC1 and of GCPII in the rat peripheral nervous system. J Anat. 2008; 213:539–546. [PubMed: 19014361]

Cerbai F, Lana D, Nosi D, Petkova-Kirova P, Zecchi S, Brothers HM, Wenk GL, Giovannini MG. The neuron-astrocyte-microglia triad in normal brain ageing and in a model of neuroinflammation in the rat hippocampus. PLoS One. 2012; 7:e45250. [PubMed: 23028880]

Chen Y, Swanson RA. Astrocytes and brain injury. J Cereb Blood Flow Metab. 2003; 23:137–149. [PubMed: 12571445]

Choi DW. Ionic dependence of glutamate neurotoxicity. J Neurosci. 1987; 7:369–379. [PubMed: 2880938]

Choi DW. Glutamate neurotoxicity and diseases of the nervous system. Neuron. 1988; 1:623–634. [PubMed: 2908446]

Choi DW. Excitotoxic cell death. J Neurobiol. 1992; 23:1261–1276. [PubMed: 1361523]

Citri A, Malenka RC. Synaptic plasticity: multiple forms, functions, and mechanisms. Neuropsychopharmacology. 2008; 33:18–41. [PubMed: 17728696]

Conway RE, Joiner K, Patterson A, Bourgeois D, Rampp R, Hannah BC, McReynolds S, Elder JM, Gilfilen H, Shapiro LH. Prostate specific membrane antigen produces pro-angiogenic laminin peptides downstream of matrix metalloprotease-2. Angiogenesis. 2013; 16:847–860. [PubMed: 23775497]

D'Onofrio M, Cuomo L, Battaglia G, Ngomba RT, Storto M, Kingston AE, Orzi F, De Blasi A, Di Iorio P, Nicoletti F, Bruno V. Neuroprotection mediated by glial group-II metabotropic glutamate receptors requires the activation of the MAP kinase and the phosphatidylinositol-3-kinase pathways. Journal of neurochemistry. 2001; 78:435–445. [PubMed: 11483646]

Danbolt NC. Glutamate uptake. Prog Neurobiol. 2001; 65:1–105. [PubMed: 11369436]

De Simone R, Niturad CE, De Nuccio C, Ajmone-Cat MA, Visentin S, Minghetti L. TGF-beta and LPS modulate ADP-induced migration of microglial cells through P2Y1 and P2Y12 receptor expression. Journal of neurochemistry. 2010; 115:450–459. [PubMed: 20681951]

Derrick M, Luo NL, Bregman JC, Jilling T, Ji X, Fisher K, Gladson CL, Beardsley DJ, Murdoch G, Back SA, Tan S. Preterm fetal hypoxia-ischemia causes hypertonia and motor deficits in the neonatal rabbit: a model for human cerebral palsy? J Neurosci. 2004; 24:24–34. [PubMed: 14715934]

Dong XX, Wang Y, Qin ZH. Molecular mechanisms of excitotoxicity and their relevance to pathogenesis of neurodegenerative diseases. Acta Pharmacol Sin. 2009; 30:379–387. [PubMed: 19343058]

Eddleston M, Mucke L. Molecular profile of reactive astrocytes--implications for their role in neurologic disease. Neuroscience. 1993; 54:15–36. [PubMed: 8515840]

Eixarch E, Batalle D, Illa M, Munoz-Moreno E, Arbat-Plana A, Amat-Roldan I, Figueras F, Gratacos E. Neonatal neurobehavior and diffusion MRI changes in brain reorganization due to intrauterine growth restriction in a rabbit model. PLoS One. 2012; 7:e31497. [PubMed: 22347486]

Endo F, Komine O, Fujimori-Tonou N, Katsuno M, Jin S, Watanabe S, Sobue G, Dezawa M, Wyss-Coray T, Yamanaka K. Astrocyte-derived TGF-beta1 accelerates disease progression in ALS mice by interfering with the neuroprotective functions of microglia and T cells. Cell Rep. 2015; 11:592–604. [PubMed: 25892237]

Erecinska M, Silver IA. Metabolism and role of glutamate in mammalian brain. Prog Neurobiol. 1990; 35:245–296. [PubMed: 1980745]

Falahati S, Breu M, Waickman AT, Phillips AW, Arauz EJ, Snyder S, Porambo M, Goeral K, Comi AM, Wilson MA, Johnston MV, Fatemi A. Ischemia-induced neuroinflammation is associated with disrupted development of oligodendrocyte progenitors in a model of periventricular leukomalacia. Dev Neurosci. 2013; 35:182–196. [PubMed: 23445614]

Farina C, Aloisi F, Meinl E. Astrocytes are active players in cerebral innate immunity. Trends in immunology. 2007; 28:138–145. [PubMed: 17276138]

Flanders KC, Ren RF, Lippa CF. Transforming growth factor-betas in neurodegenerative disease. Prog Neurobiol. 1998; 54:71–85. [PubMed: 9460794]

Floyd CL, Gorin FA, Lyeth BG. Mechanical strain injury increases intracellular sodium and reverses Na+/Ca2+ exchange in cortical astrocytes. Glia. 2005; 51:35–46. [PubMed: 15779085]

Folkerth RD. Neuropathologic substrate of cerebral palsy. J Child Neurol. 2005; 20:940–949. [PubMed: 16417840]

Foss CA, Mease RC, Cho SY, Kim HJ, Pomper MG. GCPII imaging and cancer. Curr Med Chem. 2012; 19:1346–1359. [PubMed: 22304713]

Fuhrman S, Palkovits M, Cassidy M, Neale JH. The regional distribution of N-acetylaspartylglutamate (NAAG) and peptidase activity against NAAG in the rat nervous system. J Neurochem. 1994; 62:275–281. [PubMed: 8263527]

Georgiadis P, Xu H, Chua C, Hu F, Collins L, Huynh C, Lagamma EF, Ballabh P. Characterization of acute brain injuries and neurobehavioral profiles in a rabbit model of germinal matrix hemorrhage. Stroke. 2008; 39:3378–3388. [PubMed: 18845808]

Ghadge GD, Slusher BS, Bodner A, Canto MD, Wozniak K, Thomas AG, Rojas C, Tsukamoto T, Majer P, Miller RJ, Monti AL, Roos RP. Glutamate carboxypeptidase II inhibition protects motor neurons from death in familial amyotrophic lateral sclerosis models. Proc Natl Acad Sci U S A. 2003; 100:9554–9559. [PubMed: 12876198]

Giulian D, Baker TJ. Characterization of ameboid microglia isolated from developing mammalian brain. J Neurosci. 1986; 6:2163–2178. [PubMed: 3018187]

Grady MS, Charleston JS, Maris D, Witgen BM, Lifshitz J. Neuronal and glial cell number in the hippocampus after experimental traumatic brain injury: analysis by stereological estimation. J Neurotrauma. 2003; 20:929–941. [PubMed: 14588110]

Hamberger A, Nystrom B. Extra- and intracellular amino acids in the hippocampus during development of hepatic encephalopathy. Neurochem Res. 1984; 9:1181–1192. [PubMed: 6504234]

Hardingham GE, Bading H. The Yin and Yang of NMDA receptor signalling. Trends Neurosci. 2003; 26:81–89. [PubMed: 12536131]

Haugeto O, Ullensvang K, Levy LM, Chaudhry FA, Honore T, Nielsen M, Lehre KP, Danbolt NC. Brain glutamate transporter proteins form homomultimers. J Biol Chem. 1996; 271:27715–27722. [PubMed: 8910364]

Henrich-Noack P, Prehn JH, Krieglstein J. TGF-beta 1 protects hippocampal neurons against degeneration caused by transient global ischemia. Dose-response relationship and potential neuroprotective mechanisms. Stroke. 1996; 27:1609–1614. discussion 1615. [PubMed: 8784137]

Hovelso N, Sotty F, Montezinho LP, Pinheiro PS, Herrik KF, Mork A. Therapeutic potential of metabotropic glutamate receptor modulators. Curr Neuropharmacol. 2012; 10:12–48. [PubMed: 22942876]

Huang Y, Zhao L, Jia B, Wu L, Li Y, Curthoys N, Zheng JC. Glutaminase dysregulation in HIV-1-infected human microglia mediates neurotoxicity: relevant to HIV-1-associated neurocognitive disorders. J Neurosci. 2011; 31:15195–15204. [PubMed: 22016553]

John GR, Lee SC, Brosnan CF. Cytokines: powerful regulators of glial cell activation. The Neuroscientist: a review journal bringing neurobiology, neurology and psychiatry. 2003; 9:10–22.

Johnston MV. Excitotoxicity in perinatal brain injury. Brain Pathol. 2005; 15:234–240. [PubMed: 16196390]

Johnston MV, Hoon AH Jr. Cerebral palsy. Neuromolecular Med. 2006; 8:435–450. [PubMed: 17028368]

Kannan S, Balakrishnan B, Muzik O, Romero R, Chugani D. Positron emission tomography imaging of neuroinflammation. J Child Neurol. 2009; 24:1190–1199. [PubMed: 19745091]

Kannan S, Dai H, Navath RS, Balakrishnan B, Jyoti A, Janisse J, Romero R, Kannan RM. Dendrimer-based postnatal therapy for neuroinflammation and cerebral palsy in a rabbit model. Sci Transl Med. 2012; 4:130ra146.

Kannan S, Saadani-Makki F, Balakrishnan B, Chakraborty P, Janisse J, Lu X, Muzik O, Romero R, Chugani DC. Magnitude of [(11)C]PK11195 binding is related to severity of motor deficits in a rabbit model of cerebral palsy induced by intrauterine endotoxin exposure. Dev Neurosci. 2011a; 33:231–240. [PubMed: 21791891]

Kannan S, Saadani-Makki F, Balakrishnan B, Dai H, Chakraborty PK, Janisse J, Muzik O, Romero R, Chugani DC. Decreased cortical serotonin in neonatal rabbits exposed to endotoxin in utero. J Cereb Blood Flow Metab. 2011b; 31:738–749. [PubMed: 20827261]

Kannan S, Saadani-Makki F, Muzik O, Chakraborty P, Mangner TJ, Janisse J, Romero R, Chugani DC. Microglial activation in perinatal rabbit brain induced by intrauterine inflammation: detection with 11C-(R)-PK11195 and small-animal PET. J Nucl Med. 2007; 48:946–954. [PubMed: 17504871]

Kasischke KA, Vishwasrao HD, Fisher PJ, Zipfel WR, Webb WW. Neural activity triggers neuronal oxidative metabolism followed by astrocytic glycolysis. Science. 2004; 305:99–103. [PubMed: 15232110]

Khacho P, Wang B, Ahlskog N, Hristova E, Bergeron R. Differential effects of N-acetyl-aspartyl-glutamate on synaptic and extrasynaptic NMDA receptors are subunit- and pH-dependent in the CA1 region of the mouse hippocampus. Neurobiol Dis. 2015; 82:580–592. [PubMed: 26303888]

Koeglsperger T, Li S, Brenneis C, Saulnier JL, Mayo L, Carrier Y, Selkoe DJ, Weiner HL. Impaired glutamate recycling and GluN2B-mediated neuronal calcium overload in mice lacking TGF-beta1 in the CNS. Glia. 2013; 61:985–1002. [PubMed: 23536313]

Kou Z, VandeVord PJ. Traumatic white matter injury and glial activation: from basic science to clinics. Glia. 2014; 62:1831–1855. [PubMed: 24807544]

Kreft M, Bak LK, Waagepetersen HS, Schousboe A. Aspects of astrocyte energy metabolism, amino acid neurotransmitter homoeostasis and metabolic compartmentation. ASN Neuro. 2012:4.

Krieglstein K, Zheng F, Unsicker K, Alzheimer C. More than being protective: functional roles for TGF-beta/activin signaling pathways at central synapses. Trends in neurosciences. 2011; 34:421–429. [PubMed: 21742388]

Leonardo CC, Pennypacker KR. Neuroinflammation and MMPs: potential therapeutic targets in neonatal hypoxic-ischemic injury. J Neuroinflammation. 2009; 6:13. [PubMed: 19368723]

Leviton A, Gilles F. Periventricular leukomalacia. Arch Neurol. 1981; 38:398. [PubMed: 7236080]

Lodge PA, Sriram S. Regulation of microglial activation by TGF-beta, IL-10, and CSF-1. J Leukoc Biol. 1996; 60:502–508. [PubMed: 8864135]

Marquez J, Cardona C, Campos-Sandoval JA, Penalver A, Tosina M, Mates JM, Martin-Rufian M. Mammalian glutaminase isozymes in brain. Metab Brain Dis. 2013; 28:133–137. [PubMed: 23149879]

Martin LJ, Brambrink AM, Lehmann C, Portera-Cailliau C, Koehler R, Rothstein J, Traystman RJ. Hypoxia-ischemia causes abnormalities in glutamate transporters and death of astroglia and neurons in newborn striatum. Ann Neurol. 1997; 42:335–348. [PubMed: 9307255]

Martinez-Hernandez A, Bell KP, Norenberg MD. Glutamine synthetase: glial localization in brain. Science. 1977; 195:1356–1358. [PubMed: 14400]

Mates JM, Segura JA, Martin-Rufian M, Campos-Sandoval JA, Alonso FJ, Marquez J. Glutaminase isoenzymes as key regulators in metabolic and oxidative stress against cancer. Curr Mol Med. 2013; 13:514–534. [PubMed: 22934847]

Mazzanti M, Sul JY, Haydon PG. Glutamate on demand: astrocytes as a ready source. Neuroscientist. 2001; 7:396–405. [PubMed: 11597099]

McKenna MC. The glutamate-glutamine cycle is not stoichiometric: fates of glutamate in brain. J Neurosci Res. 2007; 85:3347–3358. [PubMed: 17847118]

Min KJ, Yang MS, Kim SU, Jou I, Joe EH. Astrocytes induce hemeoxygenase-1 expression in microglia: a feasible mechanism for preventing excessive brain inflammation. J Neurosci. 2006; 26:1880–1887. [PubMed: 16467537]

Mock B, Kozak C, Seldin MF, Ruff N, D'Hoostelaere L, Szpirer C, Levan G, Seuanez H, O'Brien S, Banner C. A glutaminase (gis) gene maps to mouse chromosome 1, rat chromosome 9, and human chromosome 2. Genomics. 1989; 5:291–297. [PubMed: 2571577]

Mulligan SJ, MacVicar BA. Calcium transients in astrocyte endfeet cause cerebrovascular constrictions. Nature. 2004; 431:195–199. [PubMed: 15356633]

Neale JH. N-acetylaspartylglutamate is an agonist at mGluR(3) in vivo and in vitro. J Neurochem. 2011; 119:891–895. [PubMed: 21740441]

Norden DM, Fenn AM, Dugan A, Godbout JP. TGFbeta produced by IL-10 redirected astrocytes attenuates microglial activation. Glia. 2014; 62:881–895. [PubMed: 24616125]

Olalla L, Gutierrez A, Campos JA, Khan ZU, Alonso FJ, Segura JA, Marquez J, Aledo JC. Nuclear localization of L-type glutaminase in mammalian brain. J Biol Chem. 2002; 277:38939–38944. [PubMed: 12163477]

Ottersen OP, Zhang N, Walberg F. Metabolic compartmentation of glutamate and glutamine: morphological evidence obtained by quantitative immunocytochemistry in rat cerebellum. Neuroscience. 1992; 46:519–534. [PubMed: 1347649]

Paglinawan R, Malipiero U, Schlapbach R, Frei K, Reith W, Fontana A. TGFbeta directs gene expression of activated microglia to an anti-inflammatory phenotype strongly focusing on chemokine genes and cell migratory genes. Glia. 2003; 44:219–231. [PubMed: 14603463]

Piani D, Spranger M, Frei K, Schaffner A, Fontana A. Macrophage-induced cytotoxicity of N-methyl-D-aspartate receptor positive neurons involves excitatory amino acids rather than reactive oxygen intermediates and cytokines. Eur J Immunol. 1992; 22:2429–2436. [PubMed: 1355433]

Pierson CR, Folkerth RD, Billiards SS, Trachtenberg FL, Drinkwater ME, Volpe JJ, Kinney HC. Gray matter injury associated with periventricular leukomalacia in the premature infant. Acta Neuropathol. 2007; 114:619–631. [PubMed: 17912538]

Prehn JH, Backhauss C, Krieglstein J. Transforming growth factor-beta 1 prevents glutamate neurotoxicity in rat neocortical cultures and protects mouse neocortex from ischemic injury in vivo. J Cereb Blood Flow Metab. 1993; 13:521–525. [PubMed: 8097519]

Puttfarcken PS, Handen JS, Montgomery DT, Coyle JT, Werling LL. N-acetyl-aspartylglutamate modulation of N-methyl-D-aspartate-stimulated [3H]norepinephrine release from rat hippocampal slices. J Pharmacol Exp Ther. 1993; 266:796–803. [PubMed: 8355209]

Rahn KA, Watkins CC, Alt J, Rais R, Stathis M, Grishkan I, Crainiceau CM, Pomper MG, Rojas C, Pletnikov MV, Calabresi PA, Brandt J, Barker PB, Slusher BS, Kaplin AI. Inhibition of glutamate carboxypeptidase II (GCPII) activity as a treatment for cognitive impairment in multiple sclerosis. Proc Natl Acad Sci U S A. 2012; 109:20101–20106. [PubMed: 23169655]

Raymond M, Li P, Mangin JM, Huntsman M, Gallo V. Chronic perinatal hypoxia reduces glutamate-aspartate transporter function in astrocytes through the Janus kinase/signal transducer and activator of transcription pathway. J Neurosci. 2011; 31:17864–17871. [PubMed: 22159101]

Roberts AB, Flanders KC, Heine UI, Jakowlew S, Kondaiah P, Kim SJ, Sporn MB. Transforming growth factor-beta: multifunctional regulator of differentiation and development. Philos Trans R Soc Lond B Biol Sci. 1990; 327:145–154. [PubMed: 1969655]

Robinson MB, Blakely RD, Couto R, Coyle JT. Hydrolysis of the brain dipeptide N-acetyl-L-aspartyl-L-glutamate. Identification and characterization of a novel N-acetylated alpha-linked acidic dipeptidase activity from rat brain. J Biol Chem. 1987; 262:14498–14506. [PubMed: 3667587]

Rojas C, Frazier ST, Flanary J, Slusher BS. Kinetics and inhibition of glutamate carboxypeptidase II using a microplate assay. Anal Biochem. 2002; 310:50–54. [PubMed: 12413472]

Rothstein JD, Dykes-Hoberg M, Pardo CA, Bristol LA, Jin L, Kuncl RW, Kanai Y, Hediger MA, Wang Y, Schielke JP, Welty DF. Knockout of glutamate transporters reveals a major role for astroglial transport in excitotoxicity and clearance of glutamate. Neuron. 1996; 16:675–686. [PubMed: 8785064]

Saadani-Makki F, Kannan S, Lu X, Janisse J, Dawe E, Edwin S, Romero R, Chugani D. Intrauterine administration of endotoxin leads to motor deficits in a rabbit model: a link between prenatal infection and cerebral palsy. Am J Obstet Gynecol. 2008; 199:651.e651–657. [PubMed: 18845289]

Saadani-Makki F, Kannan S, Makki M, Muzik O, Janisse J, Romero R, Chugani D. Intrauterine endotoxin administration leads to white matter diffusivity changes in newborn rabbits. J Child Neurol. 2009; 24:1179–1189. [PubMed: 19745090]

Sacha P, Zamecnik J, Barinka C, Hlouchova K, Vicha A, Mlcochova P, Hilgert I, Eckschlager T, Konvalinka J. Expression of glutamate carboxypeptidase II in human brain. Neuroscience. 2007; 144:1361–1372. [PubMed: 17150306]

Schachtrup C, Ryu JK, Helmrick MJ, Vagena E, Galanakis DK, Degen JL, Margolis RU, Akassoglou K. Fibrinogen triggers astrocyte scar formation by promoting the availability of active TGF-beta after vascular damage. J Neurosci. 2010; 30:5843–5854. [PubMed: 20427645]

Schousboe A, Scafidi S, Bak LK, Waagepetersen HS, McKenna MC. Glutamate metabolism in the brain focusing on astrocytes. Adv Neurobiol. 2014; 11:13–30. [PubMed: 25236722]

Sen E, Levison SW. Astrocytes and developmental white matter disorders. Ment Retard Dev Disabil Res Rev. 2006; 12:97–104. [PubMed: 16807889]

Serval V, Barbeito L, Pittaluga A, Cheramy A, Lavielle S, Glowinski J. Competitive inhibition of N-acetylated-alpha-linked acidic dipeptidase activity by N-acetyl-L-aspartyl-beta-linked L-glutamate. J Neurochem. 1990; 55:39–46. [PubMed: 2355230]

Sidoryk-Wegrzynowicz M, Wegrzynowicz M, Lee E, Bowman AB, Aschner M. Role of astrocytes in brain function and disease. Toxicol Pathol. 2011; 39:115–123. [PubMed: 21075920]

Silverstein FS, Buchanan K, Johnston MV. Perinatal hypoxia-ischemia disrupts striatal high-affinity [3H]glutamate uptake into synaptosomes. J Neurochem. 1986; 47:1614–1619. [PubMed: 2876058]

Slusher BS, Tsai G, Yoo G, Coyle JT. Immunocytochemical localization of the N-acetyl-aspartyl-glutamate (NAAG) hydrolyzing enzyme N-acetylated alpha-linked acidic dipeptidase (NAALADase). J Comp Neurol. 1992; 315:217–229. [PubMed: 1545010]

Slusher BS, Vornov JJ, Thomas AG, Hurn PD, Harukuni I, Bhardwaj A, Traystman RJ, Robinson MB, Britton P, Lu XC, Tortella FC, Wozniak KM, Yudkoff M, Potter BM, Jackson PF. Selective inhibition of NAALADase, which converts NAAG to glutamate, reduces ischemic brain injury. Nat Med. 1999; 5:1396–1402. [PubMed: 10581082]

Smith AM, Graham ES, Feng SX, Oldfield RL, Bergin PM, Mee EW, Faull RL, Curtis MA, Dragunow M. Adult human glia, pericytes and meningeal fibroblasts respond similarly to IFNy but not to TGFbeta1 or M-CSF. PLoS One. 2013; 8:e80463. [PubMed: 24339874]

Sofroniew MV. Molecular dissection of reactive astrogliosis and glial scar formation. Trends Neurosci. 2009; 32:638–647. [PubMed: 19782411]

Sofroniew MV, Vinters HV. Astrocytes: biology and pathology. Acta Neuropathol. 2010; 119:7–35. [PubMed: 20012068]

Stauch BL, Robinson MB, Forloni G, Tsai G, Coyle JT. The effects of N-acetylated alpha-linked acidic dipeptidase (NAALADase) inhibitors on [3H]NAAG catabolism in vivo. Neurosci Lett. 1989; 100:295–300. [PubMed: 2668802]

Tanaka K, Watase K, Manabe T, Yamada K, Watanabe M, Takahashi K, Iwama H, Nishikawa T, Ichihara N, Kikuchi T, Okuyama S, Kawashima N, Hori S, Takimoto M, Wada K. Epilepsy and exacerbation of brain injury in mice lacking the glutamate transporter GLT-1. Science. 1997; 276:1699–1702. [PubMed: 9180080]

Thomas AG, Corse AM, Coccia CF, Bilak MM, Rothstein JD, Slusher BS. NAALADase inhibition protects motor neurons against chronic glutamate toxicity. Eur J Pharmacol. 2003; 471:177–184. [PubMed: 12826236]

Thomas AG, Liu W, Olkowski JL, Tang Z, Lin Q, Lu XC, Slusher BS. Neuroprotection mediated by glutamate carboxypeptidase II (NAALADase) inhibition requires TGF-beta. Eur J Pharmacol. 2001; 430:33–40. [PubMed: 11698060]

Thomas AG, O'Driscoll CM, Bressler J, Kaufmann W, Rojas CJ, Slusher BS. Small molecule glutaminase inhibitors block glutamate release from stimulated microglia. Biochem Biophys Res Commun. 2014; 443:32–36. [PubMed: 24269238]

Ullian EM, Sapperstein SK, Christopherson KS, Barres BA. Control of synapse number by glia. Science. 2001; 291:657–661. [PubMed: 11158678]

Unsicker K, Flanders KC, Cissel DS, Lafyatis R, Sporn MB. Transforming growth factor beta isoforms in the adult rat central and peripheral nervous system. Neuroscience. 1991; 44:613–625. [PubMed: 1754055]

Valivullah HM, Lancaster J, Sweetnam PM, Neale JH. Interactions between N-acetylaspartylglutamate and AMPA, kainate, and NMDA binding sites. J Neurochem. 1994; 63:1714–1719. [PubMed: 7523599]

Vannucci SJ, Hagberg H. Hypoxia-ischemia in the immature brain. J Exp Biol. 2004; 207:3149–3154. [PubMed: 15299036]

Vernadakis A. Glia-neuron intercommunications and synaptic plasticity. Prog Neurobiol. 1996; 49:185–214. [PubMed: 8878303]

Verney C, Pogledic I, Biran V, Adle-Biassette H, Fallet-Bianco C, Gressens P. Microglial reaction in axonal crossroads is a hallmark of noncystic periventricular white matter injury in very preterm infants. J Neuropathol Exp Neurol. 2012; 71:251–264. [PubMed: 22318128]

Vesce S, Bezzi P, Volterra A. The active role of astrocytes in synaptic transmission. Cell Mol Life Sci. 1999; 56:991–1000. [PubMed: 11212330]

Vexler ZS, Ferriero DM. Molecular and biochemical mechanisms of perinatal brain injury. Semin Neonatol. 2001; 6:99–108. [PubMed: 11483016]

Villapol S, Gelot A, Renolleau S, Charriaut-Marlangue C. Astrocyte responses after neonatal ischemia: the yin and the yang. Neuroscientist. 2008; 14:339–344. [PubMed: 18612085]

von Bernhardi R, Ramirez G. Microglia-astrocyte interaction in Alzheimer's disease: friends or foes for the nervous system? Biol Res. 2001; 34:123–128. [PubMed: 11715204]

Wan W, Wetmore L, Sorensen CM, Greenberg AH, Nance DM. Neural and biochemical mediators of endotoxin and stress-induced c-fos expression in the rat brain. Brain Res Bull. 1994; 34:7–14. [PubMed: 8193936]

Westergaard N, Sonnewald U, Schousboe A. Metabolic trafficking between neurons and astrocytes: the glutamate/glutamine cycle revisited. Dev Neurosci. 1995; 17:203–211. [PubMed: 8575339]

Wilhelmsson U, Bushong EA, Price DL, Smarr BL, Phung V, Terada M, Ellisman MH, Pekny M. Redefining the concept of reactive astrocytes as cells that remain within their unique domains upon reaction to injury. Proceedings of the National Academy of Sciences of the United States of America. 2006; 103:17513–17518. [PubMed: 17090684]

Wroblewska B, Wroblewski JT, Pshenichkin S, Surin A, Sullivan SE, Neale JH. N-acetylaspartylglutamate selectively activates mGluR3 receptors in transfected cells. J Neurochem. 1997; 69:174–181. [PubMed: 9202308]

Zhang F, Nance E, Alnasser Y, Kannan R, Kannan S. Microglial migration and interactions with dendrimer nanoparticles are altered in the presence of neuroinflammation. J Neuroinflammation. 2016; 13:65. [PubMed: 27004516]

Zhang Z, Saraswati M, Koehler RC, Robertson C, Kannan S. A New Rabbit Model of Pediatric Traumatic Brain Injury. J Neurotrauma. 2015

Zuo D, Bzdega T, Olszewski RT, Moffett JR, Neale JH. Effects of N-acetylaspartylglutamate (NAAG) peptidase inhibition on release of glutamate and dopamine in prefrontal cortex and nucleus accumbens in phencyclidine model of schizophrenia. J Biol Chem. 2012; 287:21773–21782. [PubMed: 22570482]

Highlights

- Maternal inflammation leads to glutamate dysregulation in the fetal/newborn brain
- Glutamate carboxypeptidase II is upregulated in ‘activated’ microglia
- Inflammation results in changes in astrocyte morphology in the white matter tracts
- Intrauterine endotoxin exposure leads to decreased TGF-β1 in the newborn brain

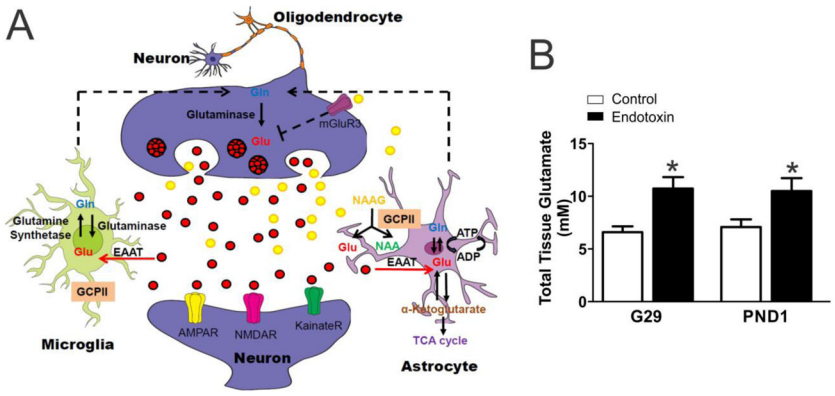

Figure 1.

Glutamate pathway and glutamate concentration. A, Schematic drawing of the glutamate pathway in neurons, microglia and astrocytes. B, Glutamate concentration is expressed as mM. Total glutamate concentration (both extracellular and intracellular glutamate) was measured in brain tissue micro-dissected from the periventricular region (Extracted from 50mg tissue in 500μL of buffer volume). Compared with the controls, the glutamate concentration was significantly increased in endotoxin kits at G29 (control=5, endotoxin=9) and PND1 (control=8, endotoxin=9). *$p<0.05$, compared with controls.

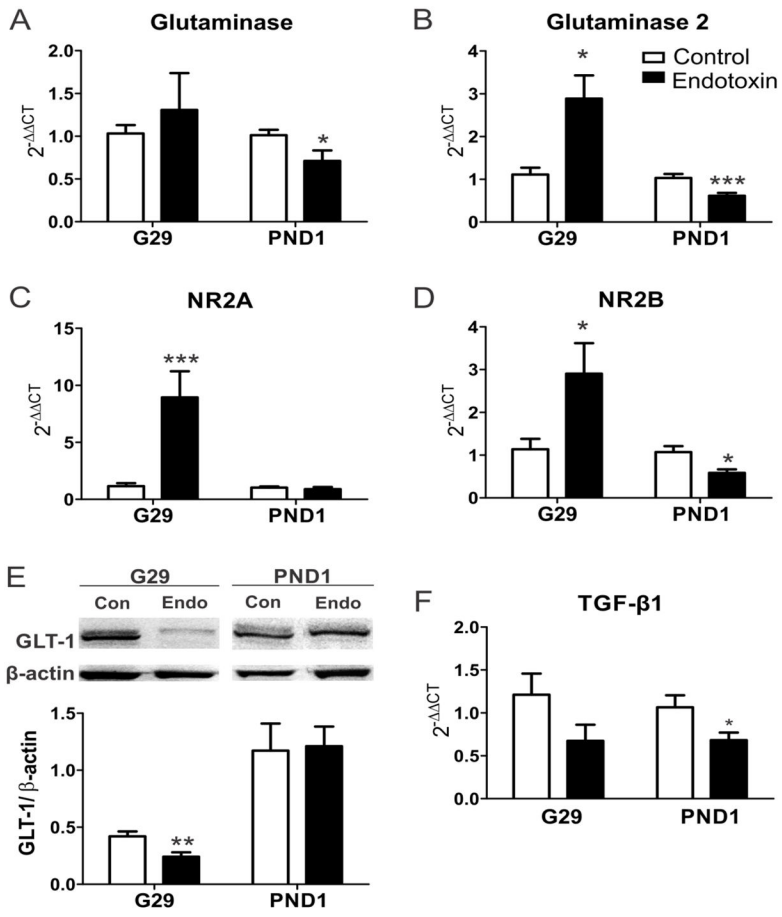

Figure 2.

A–D, In utero endotoxin exposure results in changes in mRNA expression of major glutamate enzymes and receptors. The mRNA expression of glutaminase (A), glutaminase 2 (B), NR2A (C), NR2B (D) were measured using real-time PCR. The mRNA levels of glutaminase 2, NR2A and NR2B significantly increased at G29 (1 day post-injury; control=8, endotoxin=9); the mRNA levels of glutaminase, glutaminase 2 and NR2B significantly decreased at PND1 (3 days post-injury; control=8, endotoxin=8). E, In utero endotoxin exposure leads to decreased GLT-1 protein expression in CP kits. Compared with controls, the GLT-1 protein level significantly decreased at G29 (control=8, endotoxin=9) and returned to control level at PND1 (control=8, endotoxin=9). F. The mRNA expression of TGF-β1 was significantly decreased in the CP kits at PND1 (control=8, endotoxin=8) *p<0.05, **p<0.01, ***p<0.001, compared with controls.

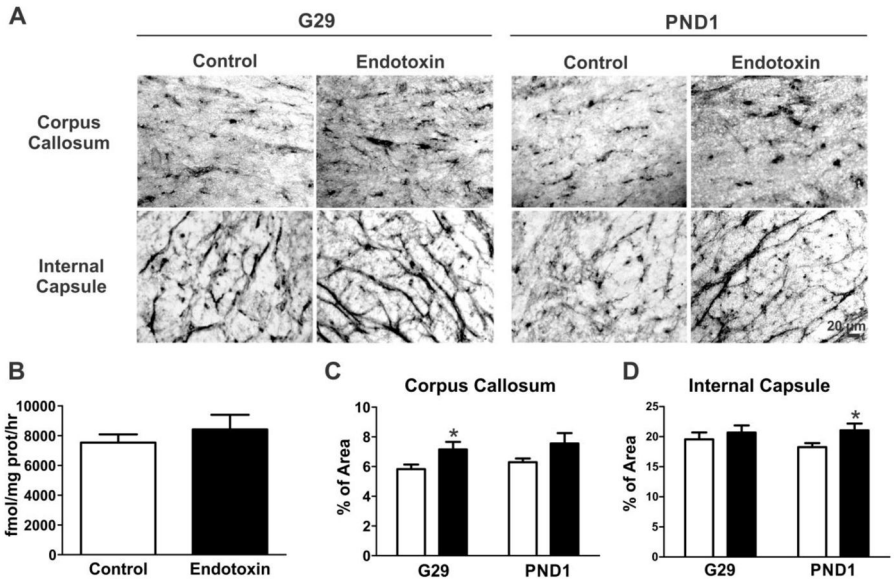

Figure 3.

GCPII expression and enzyme function at the PVR. A, Representative GCPII antibody staining images at the PVR regions from control and endotoxin kits at G29 and PND1. B, GCPII enzyme function was similar between control and endotoxin kits at PND1 (control=5, endotoxin=4). C, The percentage of area of GCPII expression significantly increased in the corpus callosum at G29 (control=5 kits, endotoxin=7kits), but no change was noted at PND1 (control=7 kits, endotoxin=5 kits). D, The percentage area of GCPII expression in the internal capsule significantly increased at PND1, but not at G29. *$p<0.05$, compared with controls. Scale bar: 20 μm.

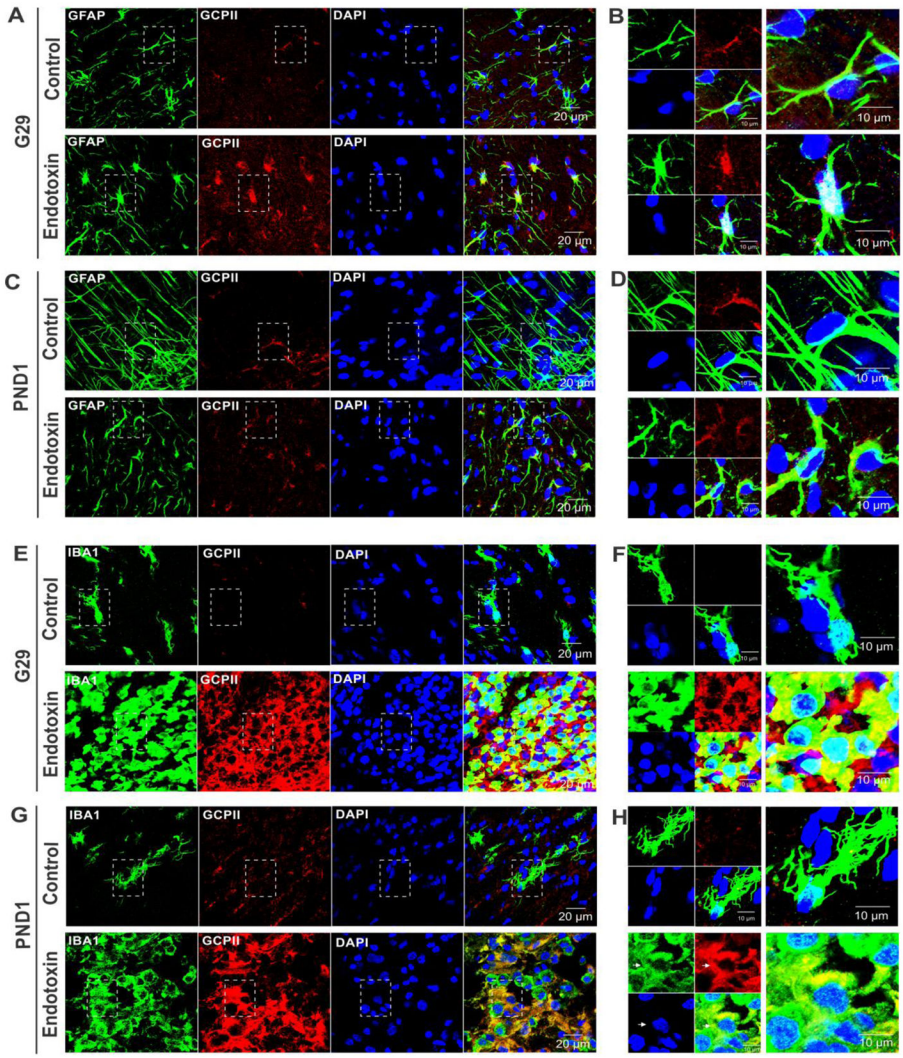

Figure 4.

Co-localization of GCPII with astrocytes and activated microglia in the PVR of CP kits. A, Representative GFAP and GCPII co-staining images from control and endotoxin kits at G29. B, The high magnification images indicated by the box in A. C, Representative GFAP and GCPII co-staining images from control and endotoxin kits at PND1. D, The high magnification images indicated by the box in C. E, Representative IBA1 and GCPII co-staining images from control and endotoxin kits at G29. F, The high magnification images indicated by the box in E. G, Representative IBA1 and GCPII co-staining images from control and endotoxin kits at PND1. H, The high magnification images indicated by the box in G. Scale bars in A,C,E,G: 20 μm. Scale bars in B,D,F,H: 10 μm. Arrows indicated some of the co-localization sites.

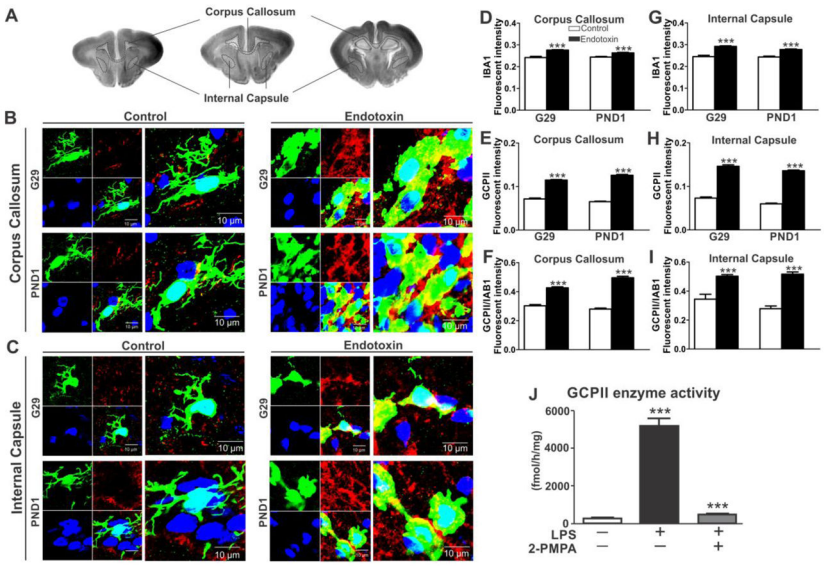

Figure 5.

GCPII expression is upregulated in activated microglia in the PVR of endotoxin kits and GCPII activity is upregulated in LPS activated rat primary microglial cells. A, Representative brain sections showing the location of the corpus callosum and internal capsule. B, Representative images of GCPII expression in activated microglia (IBA1 staining) in the corpus callosum in control and endotoxin kits at G29 and PND1. Scale bar: 10 μm. C, Representative images of GCPII expression in activated microglia (IBA1 staining) in the internal capsule in the control and endotoxin kits at G29 and PND1. Scale bar: 10 μm. D–I, The fluorescence intensity of IBA1, GCPII in IBA1 stained microglia and the ratio of the florescent intensity of GCPII/IBA1 were upregulated in the corpus callosum (D–F) and internal capsule (G–I) in endotoxin kits at both G29 and PND1. ***p <0.001. J, GCPII enzymatic activity was up-regulated in rat primary microglial cell lysates as quantified by the hydrolysis of its substrate NAA[^{3}H]G. Cells were treated for 24 h with/without LPS (1 μg/mL) and GCPII inhibitor 2-PMPA (1 μM). ***p <0.001 for LPS stimulated microglia vs. resting microglia and LPS + 2-PMPA vs. LPS.

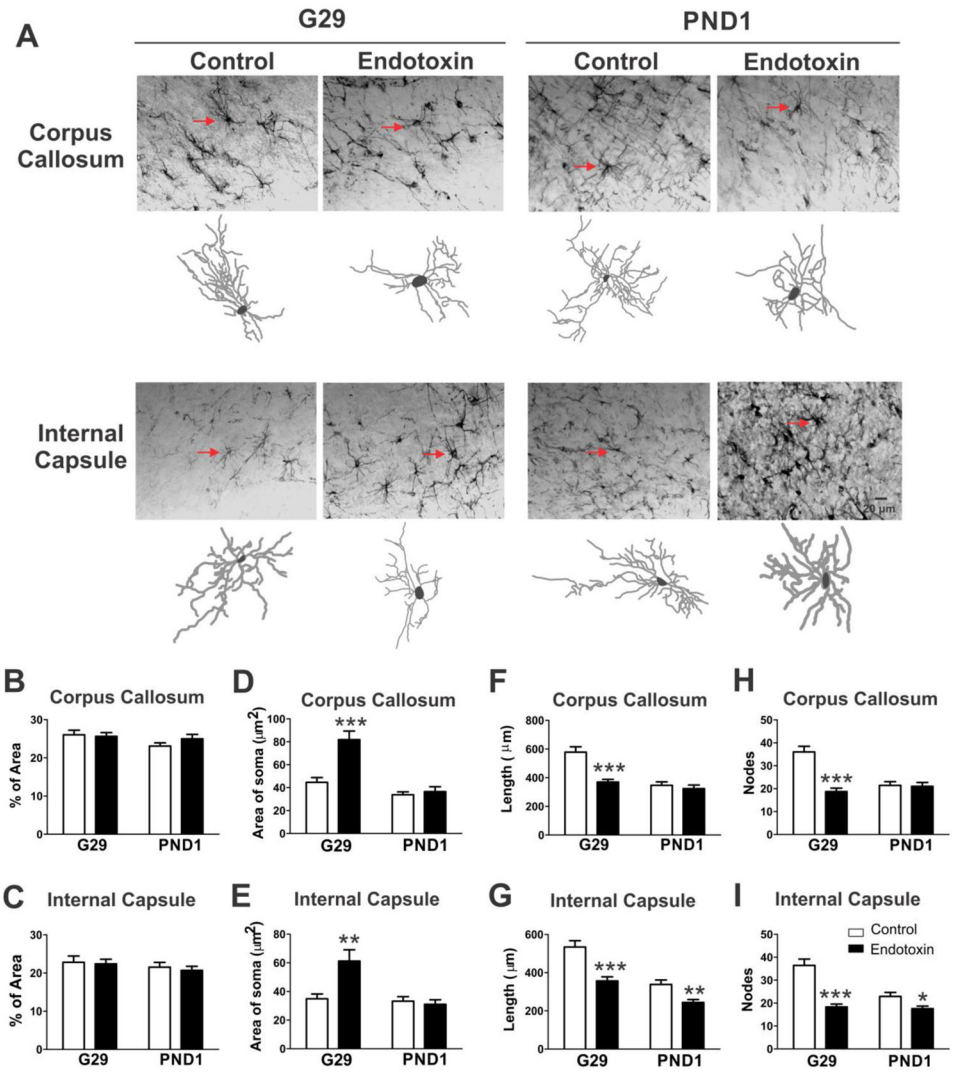

Figure 6.

In utero endotoxin exposure alters astrocytes morphology. A, Representative GFAP antibody staining images at the PVR regions from control and endotoxin kits at G29 and PND1. The Neurolucida tracing images represent the astrocytes marked with red arrows on the original images. Scale bars: 20 μm. B,C, There was no difference in the percent area of GFAP expression between control and endotoxin kits at G29 and PND1 in the corpus callosum (B) or in the internal capsule (C). D,E, The area of the soma of astrocytes in the corpus callosum (D) and internal capsule (E) was significantly larger in the endotoxin kits at G29, but not at PND1, when compared to controls. F,H The length of the processes (F) were significantly shorter and the nodes of the processes (H) were significantly decreased in the corpus callosum in endotoxin kits at G29, but not at PND1. G,I, In the internal capsule, the length of the processes (G) were significantly shorter and the nodes (I) were significantly decreased in the endotoxin kits at both G29 and PND1. *p<0.05, **P<0.01, ***P<0.001, compared with controls.

Table 1

Primers for the real-time PCR.

Gene	Accession Number	Forward primer	Reverse Primer
Glutaminase	XM_002712344.1	AGGTGGTGATCAAAGGGTAAAG	CCATGGCTGACAAAGCAAATC
Glutaminase 2	XM_002711081.1	GACGGTGGTGAACCTGTTAT	GGGAGTCGTAGTCTTTCTGTTC
NR2A	XM_002711787.1	CAAGGATCCCACGTCTACTTTC	AAGACGTGCCAGTCGTAATC
NR2B	XM_008259603.1	GGAAGAAGCCACCTACATCTTT	AGGGCACGGTATCTGTATCT
TGF-β1	XM_002722312.1	TGAGAGGTGGAGAGGAAATAGA	GGAACTGATCCCGTTGATGT
GAPDH	NM_001082253.1	TGACGACATCAAGAAGGTGGTG	GAAGGTGGAGGAGTGGGTGTC

Table 2

Neurobehavior tests scores in the control and endotoxin groups at PND1.

Behavioral scores of control and endotoxin rabbit kits on PND1. The endotoxin kits had significant impairments in locomotion and olfaction compared to control groups. Data were expressed as Median and range. P values were calculated using two-tailed unpaired t-test.

	Groups			
Outcome	**Control (n=8)**	**Endotoxin (n=8)**	**t value**	**p value**
Posture	3.0 (2.3, 3.0)	0.5 (0.1, 1.3)	6.7	< 0.0001
Suck and Swallow	3.0 (3.0, 3.0)	0.8 (0.1, 1.0)	9.3	< 0.0001
Head movement	2.5 (2.0, 3.0)	0.0 (0.0, 0.4)	9.4	< 0.0001
Forelimb movement	3.0 (3.0, 3.0)	0.5 (0.0, 1.0)	9.0	< 0.0001
Hindlimb movement	2.5 (2.1, 3.0)	0.0 (0.0, 0.4)	10.6	< 0.0001
Steps	1.0 (1.0, 1.0)	0.0 (0.0, 0.4)	7.6	< 0.0001
Aversive response to alcohol	3.0 (3.0, 3.0)	0.8 (0.5, 1.0)	10.4	< 0.0001